International Journal of New Horizon sin Physics

http://dx.doi.org/10.18576/ijnhp/050101

Effect of Reduction Temperature on Nano Structure of Thermochromic Vanadium Oxide

M. E. Hassan[1], *H. H. Afify*[2], *A. M.Badr*[1] *and H. A. Elsheikh*[1]

[1] Physics department, Aswan University, Aswan, Egypt,
[2] National research center, Cairo, Egypt.

Received: 28 Jun 2017, Revised: 1 Dec. 2017, Accepted: 2 Dec. 2017.
Published online: 1 Jan. 2018.

Abstract: The electrical properties of Vanadium Oxide thin films have long been a study because of Vanadium oxide's unique properties. Vanadium Dioxide, when heated, exhibits a sharp change in conductivity; changing from an insulating medium to a conducting or semiconductor one. This has led to its use in a number of industries, especially in the engineering fields (smart windows, heat sensors). Measurements have been made to characterize this unusual change in electrical properties, including electrical resistance, as well as XRD measurements, Surface topography by FESEM measurements. To help better understand the metal-insulator transition we have been making electrical measurements with both different Reduction time, and reduction temperature by physical vapor deposition (thermal decomposition),. The grown thin films have been deposited on glass substrate.

Keywords: Smart windows; Thermochromics; Vanadium Dioxide thin film; Thermal deposition.

1 Introduction

The building sector is one of the largest consumers of energy, especially in regions with high cooling needs such as North America, the Middle East, and Southern Europe. It is known that the cooling of buildings accounts for a large portion of the total energy consumption. Furthermore, even relatively cold regions such as that of Northern Europe experience rising needs for cooling of buildings, especially commercial buildings, largely due to the increased utilization of computers. Thermochromics (T_{Cr}) materials are of great technological interest for a variety of applications, for example in the highly interesting energy-efficient "smart windows". T_{Cr} smart windows have the potential to increase indoor comfort and save large amounts of energy for buildings and vehicles. [2,3]

The focus of this research is on VO_2-based thermochromics materials. VO_2 has a switchable infrared optical property when the temperature is changed across a critical temperature T_{cr}. It has a great potential for energy efficient fenestration, especially in hot climates. The issues that have hindered the practical applications of VO_2 in windows are the low luminous transmittance and modest solar transmittance modulation. In works covered by this thesis, a proposal for nano-thermochromics is made based on computation results which showed that VO_2-based nanoparticles can have very much improved luminous properties and solar modulation. [4]

It is well-known that VO_2 undergoes a reversible metal-to-insulator structural transition at a critical temperature T_{cr} = 68 C◦ in the bulk. At $T > T_{cr}$ VO_2 is tetragonal metallic and infrared reflecting; at $T < T_{cr}$, it is monoclinic insulating and infrared transparent. [5] This phenomenon, namely thermochromics in VO_2 was first discovered by Morin et al. To take advantage of interesting functions due to temperature-dependent switching, VO_2 has been used in various applications for sensing, and in optical communication such as in IR bolometers, photonic crystals etc., and its application as a passive switchable window glazing for energy efficient applications has also been discussed for decades. In this chapter I look into the band structure of VO_2, and discuss the advantages and problems of conventional VO_2-based films for energy efficient window applications. Finally I address the great opportunities that VO_2 nanoparticles can offer. [6, 7]

2 Experimental

Thin films of V_2O_5 have been deposited by thermal evaporation in a vacuum deposition chamber on top of Corning glass substrates. The source material (99.5% pure V_2O_5 powder RIEDEL- HAEN Ag SEELZE-HANNOVER) has been evaporated from a Molybdenum boat. The deposition pressure in the chamber has been maintained between 4×10^{-6} and 9×10^{-6} mbar and the source–substrate distance has been kept at approximately 25cm. The thermal evaporation, and post reduction has been performed using furnace (Edward 306A PVD) with a

*Correspondingauthore-mail:moh_al90@yahoo.com

ramp up of 15 K/min and a holding time of 10 min , varying the temperature between 200 °C and 300 °C (with steps of 10/min), under low pressure 10^{-3} millibar in hydrogen gas conditions. In order to control the effect of post-reduction temperature, each deposition has been performed over a batch of ten substrates from which seven samples were selected for post-reduction. The thicknesses of the films and each layer are measured by quartz crystal monitor built in the evaporation system. The structural properties of the deposited films have been diagnosed by X-ray diffractometer, Shimadzu XRD-6000, with Cu radiation λ=1.54056 Å. The X-ray tube was operated at 40 kV and 30 mA anode current throughout the measurements. XRD patterns were collected with a scanning step of 0.02◦ over the angular 2 range 10–90◦, with a total acquisition time of 15 min. The surface microstructural properties have been analyzed using scanning electron microscopy with (HRSEM) – Qunta-FEG250 system, and manufactured by Bruker. Model: MLCT-MT-A.
The electrical conductivity versus temperature has been measured in samples homemade measurement system. Critical Temperature has been determined by differentiation of the thermo-resistance hysteresis.

3 Results and discussion

3.1 X ray Diffraction

Fig.(1) show the XRD phase identification of the used substrate, which is the amorphous glass structure which are distinguished by the hump presented without any diffraction beaks. The substrates XRD chart approximately the same as in most references using glass substrate.

shows the diffraction patterns for 1st sample with thickness 80 nm, which is determined of is redacted at temperature T=200°c by quartz crystal monitor time t=10 min. there is not diffraction pattern indicate about the presence crystals of any order Vanadium oxides, this mean either still amorphous structure, the intensity of peaks are very low, due to the reduction time, and temperature.

Sample was reduced at T=300 °c for 10 min. show the strong appearance and presence of the exclusive formation of phase at V_3O_5(202) Monoclinic indicated by JCPDS file# 72-0977 standard card films is realized at2 ϑ =38.362° with cell parameters (a=9.859,b=5.0416 ,c=6.991), and week existence of monoclinic VO_2. By increasing reduction time up to 20 min. at reduction temperature T=300 °c the intensity of diffraction pattern for V_3O_5 start to decrease, the existence of VO_2 (100,011,110) monoclinic increases [JCPDS file# 71-0290], Monoclinic with cell parameters (a=9.65,b=5.8 ,c=4.5217)

Moreover, the Bragg peaks from planes with different Miller indexes and their intensity ratio correlated with those measured in reference.[10],

$$n\lambda = 2d \sin(\theta) \quad (1)$$

By considering that the broadening of Bragg peaks results from pure size effects, the crystal sizes were directly deduced from the full width at half maximum (β_{hkl}) of the peaks. [8,9]

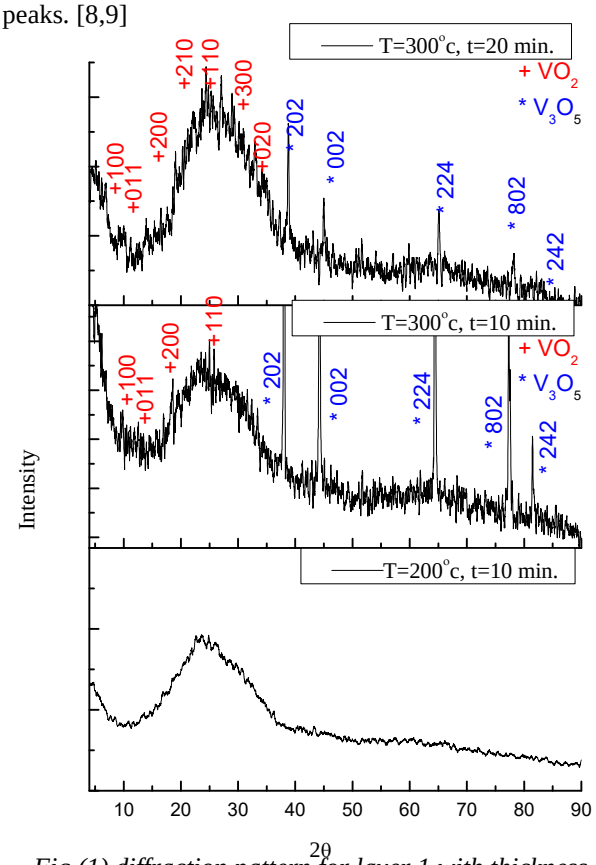

Fig (1) diffraction pattern for layer 1 with thickness 80 nm, reduction temperature and time via written on each temperature

3.2 Electrical resistance

The variation in the electrical resistance of the three films as a function of temperature and its differentiate is shown in Fig (2, 3, 4).Each plot displays a sharp change in resistance, characteristic of the insulator or semiconductor-to-metal phase transition in V_3O_5 that occurs at about 177°C , at fig(2-B) there are to transition temperature T_{cr}=184,215 °c, The change in resistance, while reversible, is accompanied by a temperature hysteresis, DTh, which is defined as the difference between the T_{cr} values measured during the heating and cooling cycles; the size of DTh varies from sample to sample.

Upon heating above room temperature, a rather sharp S–M transition occurs at 184, 215 °C, while an equally sharp M–S transition occurs upon cooling at 172,205°C with DTh= 10 °C. Such hysteretic behavior is characteristic of normal order phase transitions for sample reduced at temperature T=200°C for 10 min. with the increasing of Reduction temperature up to 300°C for 10 min as at fig(3-A,B) S–M transition occurs at 185°C, while an equally sharp M–S transition occurs upon cooling at 184°C with DTh= 1 °C.

Such hysteretic behavior is characteristic of first order phase transitions for sample reduced**.** [11]

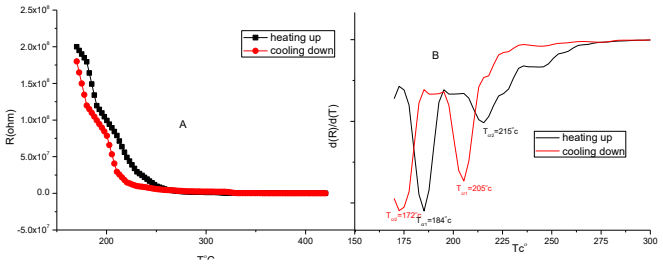

Fig (2) Reduction temperature T=200 °c for 10 min A electrical resistance, B differentiate of electrical resistance

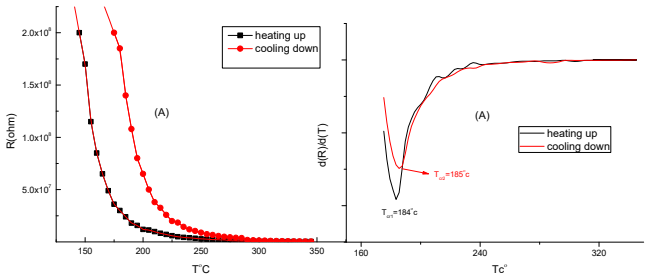

Fig (3) Reduction temperature T=300 °c for 10 min A electrical resistance, B differentiate of electrical resistance

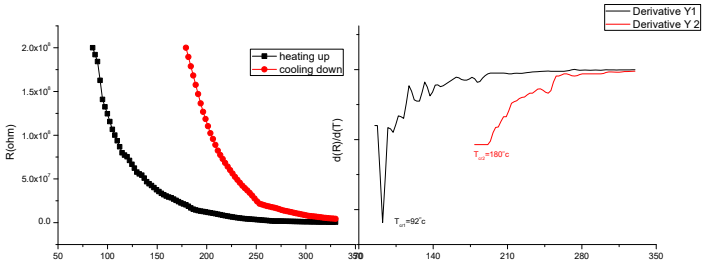

Fig (4) Reduction temperature T=300 °c for 20 min A electrical resistance, B differentiate of electrical resistance

Fig(4) represent the transition to the metallic phase, the resistance decreases exponentially with increasing temperature in the semiconducting low temperature (monoclinicVO_2, V_3O_5) mixed phase, reflecting activation energy for conduction (E_a) 0.0175 eV for the films VO_2 Monoclinic, which will be tetragonal phase after transition temperature for sample reduced at T=300°C for 20 min. it is obvious that the existence of Monoclinic VO_2 reduced the metal- semiconductor transition temperature in compression with the previous two cases at fig(2,3). The critical temperature T_{cr} decreased to 92°C by increasing reduction time and temperature up to 300°C for 10 min as in fig (4-b).

3.3 surface morphology

To further detect the microstructure, and nanostructure of the composite film, high resolution scanning electron microscopy (HRSEM). As shown in Fig. 5 (A), the film is randomly oriented with small amount of film primary composed of at the wright positioning at reduction temperature T=200°C for 10 min, Fig. 5 (B) micrographs of the film, , indicate that crystallites are well formed with the increasing of Reduction temperature up to 300°C for 10 min. From these micrographs, the distribution of grain sizes of V_3O_5 film deposited has been oriented and composed as Nano sphere like with average diameter 95 nm measured. By increasing reduction time up to 20 min. at reduction temperature T=300°C the compositions of high homogenously fine structure of Nano sphere like at fig (5-C).

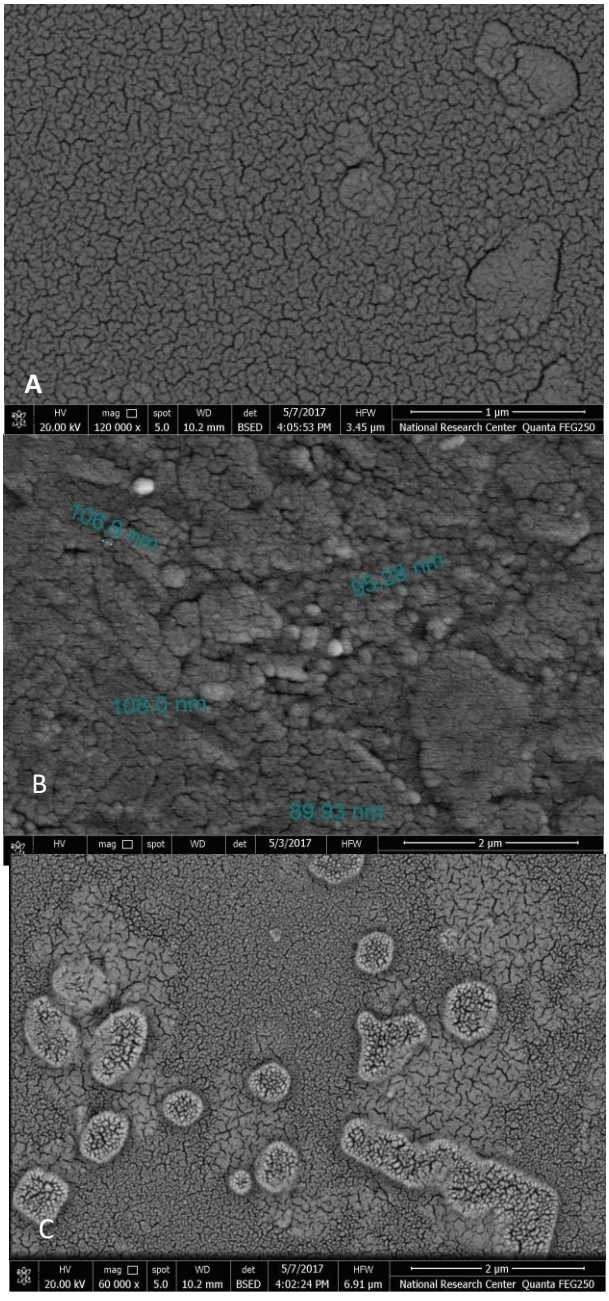

Fig (5) surface morphology scanned by high resolution SEM, (A, B, C) are corresponding about reduction temperatures and times (200°C-10 min, 300°C-10 min, 300°C-20 min

4 Conclusions

By increasing the reduction time, and temperature the existence and the crystallization of VO_2 increase and its existence increases, which are decreasing the metal semiconductor transition temperature T_{cr}. Also Nano compositions start to appear, with high homogenously surface morphology, at the reduction in hydrogen gas at low pressure.

References

[1] Troy D. Manning, Ivan P. Parkin, Christopher Blackman and Uzma Qureshi.

[2] M. Gurvitch, S. Luryi, A. Polyakov and A. Shabalov, M. Dudley, G. Wang, and S. Ge, V. Yakovlev, JOURNAL OF APPLIED PHYSICS 102, 033504 2007.

[3] Marta Ibisate1, Dolores Golmayo and Cefe L´opez, JOURNAL OF OPTICS A: PURE AND APPLIED OPTICS, J. Opt. A: Pure Appl. Opt. 10 (2008) 125202 (6pp)

[4] Carlos Batista, Ricardo M Ribeiro and Vasco Teixeira, Nanoscale Research Letters 2011.

[5] Lili Zhao, Lei Miao, Chengyan Liu, Chengyan Liu, Toru Asaka, Yipu Kang, Yuji Iwamoto, Sakae Tanemura, Hui Gu, Huirong Su, Surfaces interfacesand thinfilms, Novemeber 2011.

[6] M. B. Sahana, M. S. Dharmaprakash and S. A. Shivashankar Journal of Matrial chemestry Decmber 2001.

[7] Z. Yang,C. Ko, and S. Ramanathan, JOURNAL OF APPLIED PHYSICS 108, 073708 -2010.

[8] V. Melnik, I. Khatsevych, V. Kladko, A. Kuchuk, V. Nikirin , B. Romanyuk, Materials Letters 68 (2012) 215–217

[9] J.-C. Valmalette, J.-R. Gavarri, Materials Science and Engineering B54 (1998) 168–173.

[10] Xiaochun Wu, Fachun Lai, Limei Lin, Yongzeng Li, Lianghui Lin, Yan Qu, Zhigao Huang, Applied Surface Science 255 (2008) 2840−2844.

[11] Jongsun Maeng, Tae-Wook Kim, Gunho Jo, Takhee Lee, Materials Research Bulletin 43 (2008) 1649–1656.